low thermal gradients correspond with areas of high sand percentage, primarily because sands are better conductors than shale and therefore show as low thermal gradients[9].

1. Thermal conductivity varies with depth due to variable lithology and water content, from 8 W/mk in the Benin Formation to 5 W/mk in the marine shale formation.
2. Thermal conductivity calculations were based on assumed matrix conductivity of sand 6.1 W/mk and shale 2.1 W/mk, predominant lithologies in the Niger Delta.
3. Heat flow derived from thermal conductivity estimates at the central part of the Delta is 20–30 mW/m^2, it increases both seaward and northward to (40–55 mW/m^2).
4. Thermal conductivity decreases with increase in temperature.
5. Thermal conductivity contrast between rock types is a shallow phenomenon.
6. Heat flow corresponds to variations in geothermal gradient.

1. Akpabio, I. O. and Ejedawe, J. E., Temperature variations in the Niger delta subsurface from continuous temperature logs. *Global J. Pure Appl. Sci*., 2001, **7**, 137–142.
2. Norden, B. and Forster, A., Thermal conductivity and radiogenic heat production of sedimentary and magmatic rocks in the Northeast German Basin. *AAPG Bull*., 2006, **90**, 939–962.
3. Majorowicz, J., Jessop, A., Lane, A. M. and Larry, S., Regional heat flow pattern and lithospheric geotherms in Northeastern British Columbia and adjacent northwest territories, Canada. *Bull. Can. Pet. Geol.*, 2005, **53**, 51–66.
4. Reijers, T. J. A., Petters, S. W. and Nwajide, C. S., The Niger Delta basin. In *African Basins, Sedimentary Basins of the World* (ed. Selley, R. C.), 1997, vol. 3, pp. 145–172.
5. Schlumberger, *Log Interpretations, Principles and Applications*, Schlumberger Education Services, Houston, Texas, 1989.
6. Chapman, D. S., Keho, T. H., Bauer, M. S. and Picard, M. D., Heat flow in the Uinta Basin determined from BHT data. *Geophysics*, 1984, **49**, 453–466.
7. Briguad, F., Chapman, D. S. and Douaran, S. L., Estimating thermal conductivity in sedimentary basins using lithologic data and geophysical well logs. *AAPG*, 1990, **74**, 1459–1477.
8. Ejedawe, J., LITHTEMP, pers comm. Exploration Department, Shell Petroleum Development Company, Warri, 1997.
9. Akpabio, I. O., Ejedawe, Ebeniro, J. O. and Uko, E. D., Geothermal gradients in the Niger delta basin from Continuous temperature logs. *Global J. Pure Appl. Sci*., 2003, **9**, 265–272.
10. Zielinski, G. W., Bjoroy, M., Zielinski, R. L. B. and Ferriday, I. L., Heat flow and surface hydrocarbons on the Brunei continental margin. *AAPG Bull.*, 2007, **91**, 1053–1080.
11. Berge, P. A., Bomer, B. P. and Berryman, J. G., Ultrasonic velocity porosity relationship for sandstones analog made from fused glass beads. *Geophysics*, 1995, **60**, 108–119.
12. Kim Hyoung, C. and Lee Youngmin, Heat flow in the Republic of Korea. *J. Geophys. Res*., 2007, **112**, B05413.
13. Pribnow, D. and Umsonst, T., Estimation of thermal conductivity from the mineral composition: influence of fabric and anisotropy, *Geophys. Res. Lett.*, 1993, **20**, 2199–2202.
14. Davies, M. G., Chapman, D. S., Wagoner, T. M. Van and Armstrong, P. A., Thermal conductivity anisotropy of metasedimentary and igneous rocks. *J. Geophys. Res*., 2007, **112**, B05216.
15. Pilkington, M., Miles, W. F., Ross, G. M. and Roest, W. R., Potential-field signatures of buried Precambrian basement in the Western Canada Sedimentary Basin. *Can. J. Earth Sci.*, 2000, **37**, 1453–1471.

ACKNOWLEDGEMENT. We thank the SPDC, Nigeria for allowing the use of their facilities and access to the data on which this study was based.

Received 8 July 2008; revised accepted 30 September 2009

Comparative assessment of micro-watershed silt load with morphological parameters to evaluate soil conservation strategies

Praveen G. Saptarshi* and Rao Kumar Raghavendra

Department of Environmental Sciences, University of Pune, Pune 411 007, India

The comparative assessment of morphologic runoff and annual silt load from micro-watersheds can help in establishing relationships between these parameters with objectives of controlling runoff, conservation of soil, reduction of reservoir silt load and enhanced groundwater resources in the micro-watersheds. The automated watershed delineation technique using the filled digital elevation model is observed to be reliable for area having converging slopes. The estimation of watershed based annual silt load using universal soil loss equation along with runoff estimation utilizing the soil conservation services model using remote sensing data is possible on such automatically delineated micro-watershed groups. This can be validated through ground measurements. The output in raster geographic information system (GIS) is highly beneficial in making an inventory of soil loss, runoff and morphologic parameters with an objective of establishing relationship between these parameters for planning conservation measures. The GIS output products like soil-erosion potential map, run-off potential map, etc. obtained by using raster interpolation techniques are of value addition for developing and harnessing natural resources enabling sustainable development.

Keywords: Automated watershed delineation, comparative assessment, morphologic parameters, peak runoff, rainfall intensity, soil erosion, surface interpolation.

LAND evaluation is necessary to assess the potential constraints of a given piece of land[1]. Watershed approach is

*For correspondence. (e-mail: pgsaptarshi@unipune.ernet.in)

considered to be effective in the fragile and heterogeneous ecosystem[2]. Raster analysis in GIS can help in automatically delineating the micro-watershed groups based on a specified threshold to be decided based on the size of micro-watersheds to be delineated. Many scientists proposed algorithms for the processing of the digital elevation model (DEM) for delineating the micro-watersheds. Band[3] used DEM to identify concave and convex surfaces. Different methods for assigning flow directions in the flat areas or sinks have been proposed. DEM generated by different algorithms have been tested for accuracy of slope maps[4]. The accuracy of the DEM derived by using interpolation when applied to the residual area tends to have less slope variations and has problems of depression and flat area[5]. The algorithms given by Martz and Garbrecht[6] are best suitable, however they tend to produce parallel flows in the flow accumulation layer derived using the flow direction layer[7]. The lack of detailed elevation data can generalize the terrain undulations, which can lead to automated delineation of micro-watersheds having unrealistic shapes, thereby requiring lots of modification taking into consideration many land characteristics. Land cover study, terrain evaluation for slope and estimation of soil erosion using integration of remote sensing and geographic information system (GIS) techniques along with morphologic parameter evaluation can be utilized as a comparative assessment of micro-watersheds[8]. The rainfed watersheds of the study area lie in semi-hilly terrain and soil erosion is the main threat to sustainable development. The GIS analysis can be utilized for qualitative and quantitative land evaluation of spatial variations in topographic features of the micro-watersheds[9]. Comparative assessment of morphologic parameters with runoff computed using remote sensing data adopting the soil conservation services (SCS) model and quantified annual soil loss can help in evolving action plans for conserving land and water resources in the micro-watersheds. There are number of watershed based soil erosion estimation models. The empirical universal soil loss equation (USLE) erosion prediction model is effective in GIS environment[10]. Parameters such as cropping factor, conservation factor and soil erosive factor can be arrived at using good resolution remote sensing images so as to enable collection of field point sample data appropriately for interpolating continuous raster layers pertaining to USLE process models. The MMF model for estimating the soil erosion is also used in GIS environment and is considered to be more suitable in undulating terrain. The study area has undulating terrain at its upper reaches and is generally plain towards the lower reaches where the streams converge, accordingly the USLE soil erosion model is expected to give reliable outputs in raster GIS involving integration of continuous raster layers pertaining to USLE soil erosion process model. The outputs in raster GIS analysis can be evolved using different interpolation methods to generate a continuous surface of model parameters and by integration of raster layers using mathematical functions. This would be highly beneficial in making an inventory of soil loss, runoff and morphologic parameters with an objective of establishing relationship between these parameters for planning conservation measures. In the present study, comparative assessment of morphologic parameters, runoff and annual sediment yield estimates using USLE model for all nine automatically delineated micro-watershed groups have been carried out.

The present study has been carried out in Bavdhan micro-watersheds surrounding Pune city in western Maharashtra and occupies the eastern part of Mula River basin. The micro-watersheds of the study area is located between lat. 18°30′8.74″–18°33′58.49″N and long. 73°44′50.74″–73°49′8.3″E. The total area covered by watersheds is 25.7 sq. km of this 30.5% alone is arable area whereas 42.1% is forest area. With varied climatic and topographic features, this area has a luxuriant forest cover harbouring valuable economic and medicinal plant species. The satellite data for the study is standard false colour composite (FCC) of LISS-III remotely sensed satellite data of 23.5 m spatial resolution obtained on 3 January 2001, covering the study area and topographical map 47 F/14 of 1 : 50,000 scale in polyconic projection system. The remote sensing image gives the level-I land cover details at the instant of data acquisition. The land cover has undergone alterations over the years due to anthropogenic activities, however the concept of morphological evaluation, hydrological analysis and soil erosion estimates remains the same irrespective of landscape changes since the parameter estimates can be evolved using the updated remote sensing FCC images as and when required. There are nine micro-watershed groups generated by clubbing two to six appropriate sized automatically delineated micro-watersheds. The micro-watersheds have been delineated using the eight directional flow algorithm (D-8 method) considered to be reliable in hilly and gently undulating terrain by using a threshold value of 3185 pixels for the flow accumulation layer arrived using the trial and error approach. The stream pattern of the flow accumulation layer generally corresponds with the topographical streams available in topographic maps in undulating terrain but in plain area these two stream patterns do not tally. This is because the flow accumulation layer gives an inference about the number of surrounding pixels contributing to flow at a particular pixel location, whereas the topographic streams are incised on the ground due to erosion process with good degree of orientation towards the watershed outlet in hilly areas and are not so well-oriented in plain area. This can lead to flow occurring in infinite directions, which the D-8 algorithm is not capable of handling. The threshold value governs the size of the micro-watersheds. Smaller threshold will lead to larger-sized watershed delineation whereas larger-sized threshold will lead to smaller-sized

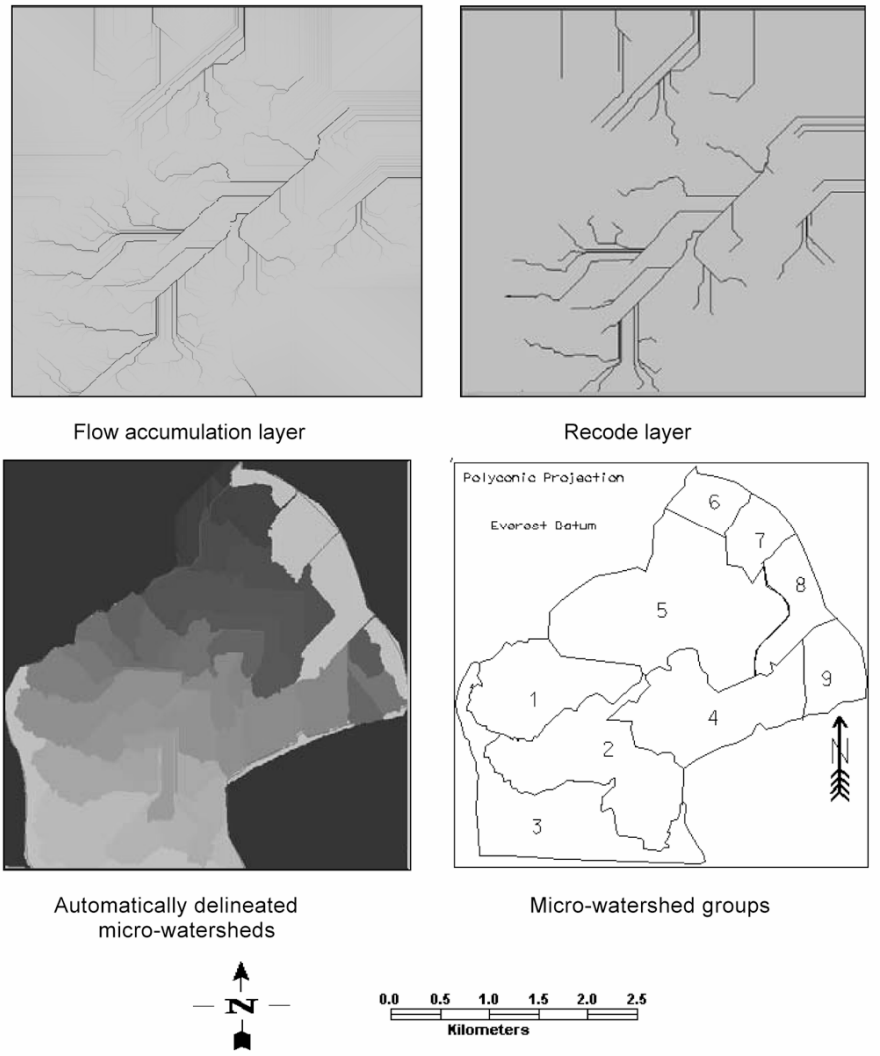

Figure 1. Automatically delineated micro-watersheds group of study area.

watersheds in the algorithm. Figure 1 shows automated micro-watersheds delineated for 3185 pixel threshold for the area along with the nine micro-watershed groups of comparable sizes varying from 1.06 to 7.6 sq. km. The nine micro-watersheds have been grouped on the basis of flow direction.

Detached sediments traversing through drainage network can lead to appreciable loss of soil fertility including rapid sedimentation of reservoirs. Accordingly, the comparative assessment of morphologic parameters with runoff estimates and quantified soil loss using the USLE model can help in establishing relationships between these parameters with objectives of controlling run-off, conservation of soil, reduction of reservoir silt load and enhanced groundwater resources in the micro-watersheds. GIS output products like erosion potential map, continuous surface interpolation techniques can be of value addition in this direction for developing and harnessing natural resources for sustainable development.

GIS analysis can be much faster and accurate compared to conventional methods[11]. The temporal variation effect on sediment yields can be approximately simulated by analysing the isolated rainstorm events[12]. The average rate of soil erosion for each feasible alternative combination of crop system and management practices in association with a specified soil type, rainfall pattern and topography can be effectively performed in GIS. When these predicted losses are compared with the given soil loss tolerance, they provide specific guidelines for effecting erosion control within specified limits. The remote sensing data facilitate identification of existing or potential erosion prone areas, which may help in planning reclamation or preventive measures. At the small scale of satellite imagery, only large-scale erosion prone areas can be identified directly. However, from satellite images, potential erosion prone areas can be determined indirectly from some of the features that are identified at those scales. Seasonal tonal variation caused due to change of

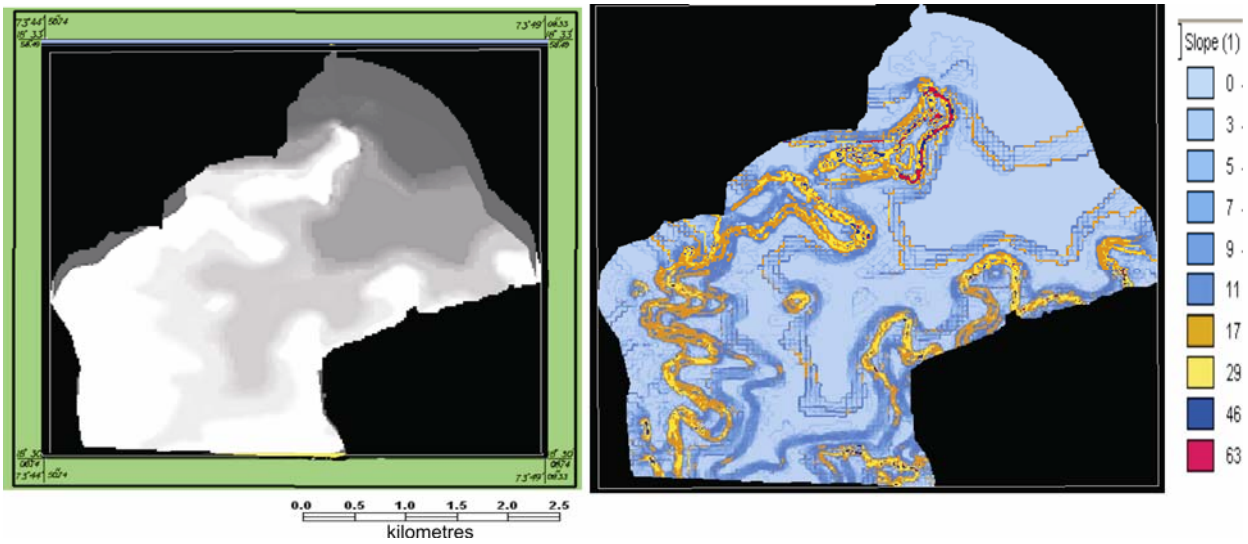

Figure 2. Raster DEM with raster slope map.

vegetation cover can be evaluated to increase the accuracy of interpretation of terrain condition.

In the present study, the micro-watersheds are delineated from DEM generated using digitized contour data obtained from topographical maps. This can generalize the slope map and ignore the localized variations. The spline local interpolation has been used to get a minimum curvature DEM and it has been improved by applying the fill depression removal algorithm[6]. Here the central lowest pixel value representing the depression in the 3×3 matrix used for processing will be raised to the lowest outflow pixel value. Figure 2 shows 2-D raster DEM at 10 m resolution and raster slope map. The DEM has been generated with a tension factor of 0.1 and the DEM has been validated at 12 locations with ground measurements using total station on a relatively flat ground for reliability of assessment. The measurements are shown in Table 1. The residual errors are within acceptable limits so the spline DEM interpolation with tension factor of 0.1 can give validated raster DEM suitable for hydrologic watershed-based analysis. In raster DEM, lighter the shade higher is the elevation, whereas in raster slope layer, red hue indicates higher slope areas, and light blue hue indicates flat slope areas.

Image classification of remote sensing data was done after reducing the correlation in spectral bands using principal component analysis (PCA). The minimum distance to mean classification on principal component composite suited the requirements of reliable land-use/land-cover output. The weighted curve number used in the SCS run-off model for every feature was obtained for different antecedent moisture condition (AMC) and the runoff values in cm depth for rainfall values obtained in cm depth along with morphologic parameters was computed using the SCS model for each micro-watershed.

USDA SCS curve number technique[13] was used for runoff computation. Image classification of 23.5 m data gave a reliable level-I details of the landscapes suitable to obtain weighted curve numbers for different periods representing different antecedent moisture conditions and hydrological soil groups[14]. The hydrological evaluation of micro-watersheds necessarily involve relating the runoff with watershed morphological parameters and quantifying the peak runoff parameter, which is useful to plan water conservation strategies including design of conservation structures. For design of water conservation structures, the peak runoff (Q_p) for small watersheds can be computed using the SCS dimensionless hydrographs for micro-watersheds[14] given by:

$$Q_p = 0.0208 * \text{area of watershed} * Q/T_p, \quad (1)$$

where T_p is the time to peak in hours, which is a function of time of concentration; Q_p the peak runoff rate in cubic metres per second; area of watershed will be in hectares, and Q the SCS runoff in cm depth.

The USLE model parameters are to be computed to cater to the local variations for reliable estimates. Geomedia Professional 6.0 raster and vector modules were used.

Table 2 gives an estimate of the rainfall erosive factor of USLE obtained by computing the kinetic energy for six storms during the rainy months from June to October for 10 year data from 1997 to 2007. The rainfall erosive factor has variation in its value due to different rainfall intensities and has been averaged monthly for the five rainy months. The monthly averaged R-value for all the storms has been averaged annually for computing the long-term USLE soil erosion estimates. Kinetic energy for each storm is given by:

Table 1. DEM validated with field total station measurements

Sample no.	Location (long., lat.) D : M : S	Elevation using total station (m) [t]	Elevation from spline interpolated DEM (m) [s]	Residual error $\|[t - s]\|$
A	73 : 46 : 18, 18 : 31 : 38	660.173	660	0.173
B	73 : 45 : 10, 18 : 30 : 20	720.286	720	0.286
C	73 : 45 : 09, 18 : 30 : 24	719.865	720	0.135
D	73 : 45 : 06, 18 : 31 : 54	740.776	741	0.224
E	73 : 47 : 13, 18 : 31 : 43	580.233	580	0.233
F	73 : 47 : 14, 18 : 32 : 49	680.337	680	0.337
G	73 : 47 : 30, 18 : 32 : 54	578.864	579	0.136
H	73 : 48 : 08, 18 : 33 : 07	560.247	560	0.247
I	73 : 48 : 51, 18 : 32 : 12	600.104	600	0.104
J	73 : 47 : 35, 18 : 33 : 37	559.913	560	0.087
K	73 : 43 : 44, 18 : 31 : 26	619.947	620	0.053
L	73 : 45 : 50, 18 : 31 : 04	660.123	660	0.123
			Average	0.183

Table 2. USLE averaged *R*-value

Averaged *R*-value (June)	Averaged *R*-value (July)	Averaged *R*-value (August)	Averaged *R*-value (September)	Averaged *R*-value (October)
2.29	5.6	5	159.8	0.1
2.89	77.25	0.42	0.416	7.6
3.82	71	2.13	4.11	10.2
11.93	27	22.18	0.18	35
43.7	27.5	76.61	2.03	33.4
140.8	101.9	29.67	0.18	5.1
R-value (averaged) = 34.23833	*R*-value (averaged) = 51.70833	*R*-value (averaged) = 21.268	*R*-value (averaged) = 27.786	*R*-value (averaged) = 15.23333

$$E_j = 0.119 + 0.0873 \log_{10} i_j, \quad (2)$$

for $i_j < 76$ mm/h, and $E_j = 0.283$ for $i_j > 76$ mm/h, E_j is the kinetic energy in mega joules/ha/mm of rainfall.

Average annual for all storms averaged over the five rainy months for 10 years from 1997 to 2007 for the rainfall data collected in the area 30.0468.

The soil erosive factor (K) depends on physiographic cum soil map of the watershed. The soil maps are prepared by using standard FCC of preferably summer season to delineate physiographic map units. It is necessary to collect soil samples randomly all over the study area to establish correlation between the soil physiographic form and soil type with correct stipulation of soil composition of map units. In order to prevent significant influence of vegetation (especially agricultural) that tends to impede the soil mapping process, summer season data is a natural choice. However, access to the complimentary data containing greenery is always helpful due to reflection of soil moisture and its field capacity in the greenery of the vegetation.

The *K*-factor in the USLE relates to the rate at which different soils erode, it signifies the resistance of the soil to both detachment and transport, and it varies with soil texture, aggregate stability, infiltration capacity and organic and chemical constituents. A simple graph has been developed to arrive at the value of '*K*'. Only five soil parameters need to be known for utilizing the graph like per cent silt plus very fine sand, per cent sand greater than 0.10 mm, organic matter content, structure and permeability. The graph is effective for the study area lying in western Maharashtra and its surroundings. The *K*-factor is obtained at sampled locations in the watershed depending upon the variability of soil type as determined from soil maps or remote sensing data (FCC). The *K*-factor obtained at different sample locations can be interpolated at unsampled locations for obtaining *K*-map for use in GIS.

Table 3 gives the value of *K* computed from the graph after collecting eight soil samples and analysing their properties in the laboratory.

The parameter *C* and to certain extent *P* values can be evaluated based on land-use/land-cover information derived from remote sensing data. *C*-value computation has been done at various locations, which undergo seasonal variations. The soil loss ratio under barren and under vegetation cover is obtained through temporal satellite data analysis and the weighted *C*-value has been computed at the chosen sample sites and shown in Table 4. It is observed that generally when cultivation is carried out in sloping soil exposed to erosive rain, the protection offered by the sod or the close growing crops in the system needs to be supported by practices that will slow the run-

off and thus reduce the amount of soil it will carry. The most important of these supporting practices are contour cultivation, strip cropping, terracing system and waterways for disposal of excess rainfall. Factor *P* in USLE is the ratio of soil loss with a specific supporting practice to the corresponding loss with the up and down cultivation. Its effectiveness varies according to the slope of the land. Contour cultivation is most effective on middle range slopes from 2% to 8% and less effective on flatter slopes and steeper slopes. There are no organized conservation measures in the area so the *P*-value has been taken as unity for all the nine micro-watersheds.

The slope length factor and the slope steepness factor are combined in a single index. The appropriate value are obtained using:

$$LS = \sqrt{L}\,(0.136 + 0.097S + 0.0139S^2)/100, \quad (3)$$

where *L* is in m and *S* in per cent.

$$L = (0.5 * D_A)/L_{CH}, \quad (4)$$

where D_A is the drainage area in sq. m, L_{CH} the total length of channels in the watershed in m.

The average slope of watershed (*S*) is obtained from the topographic map of watershed by using the following formula:

$$S = (M * N)/A * 100, \quad (5)$$

Table 3. *K*-value computed from the graph after collecting eight soil samples

Soil sample no.	*K*-value	Location	Micro-watershed no.
1	0.3	73 : 47 : 26, 18 : 32 : 52	5
2	0.33	73 : 47 : 54, 18 : 31 : 31	4
3	0.35	73 : 45 : 39, 18 : 31 : 08	2
4	0.39	73 : 46 : 45, 18 : 31 : 07	2
5	0.41	73 : 48 : 10, 18 : 32 : 50	8
6	0.36	73 : 46 : 04, 18 : 32 : 18	5
7	0.42	73 : 45 : 42, 18 : 30 : 32	3
8	0.34	73 : 47 : 42, 18 : 33 : 31	6

Table 4. Weighted *C*-value averaged

C-sample site no.	*C*-value	Micro-watershed no.
1	0.87	3
2	0.75	2
3	0.80	1
4	0.92	5
5	0.90	4
6	0.78	6
7	0.87	7
8	0.80	8
9	0.82	9

where *S* is the per cent average watershed slope, *M* the total length of contours within the watershed in m, *N* the contour interval in m and *A* the size of watershed in sq. m. The *LS* factor for the micro-watersheds are shown in Table 5.

Raster GIS analysis was performed by creating raster continuous surfaces for the five USLE point parameters utilizing the kriging interpolation tools in GIS and the raster layers were integrated to evolve the total sediment load from each micro-watershed to enable its prioritization. Figure 3 shows the raster USLE parameter layers obtained for the USLE parameters at 5 m resolutions. Comparative evaluation was performed between the morphological parameters, SCS runoff/peak runoff and soil load for each micro-watershed to enable planning of conservation strategies. A concept towards this for sediment yield prediction for watershed for suitable action plan is shown in Figure 4.

The SCS model runoff was calculated for all nine watershed groups using maximum value annual average rainfall of 1338.2 mm after collecting the rainfall data for 10 year period between 1997 and 2006. Table 6 gives the different morphologic parameters, SCS runoff (cm) and peak runoff rate (cumec) for all the nine micro-watersheds. Trends of increase in runoff with increase of drainage density have been observed. Morphologic parameters control the runoff process. Intensities of rainfall in the area for different storm data collected for the area vary between 0.1 and 225 mm/h. The average value of rainfall intensity in the area ranges between 25 and 40 mm/h. The USLE based annual silt load for the nine micro-watersheds is given in Table 7. The annual silt load varies from 6.4 to10.7 tonnes per hectare per year.

Micro-watershed no. 2 has excessive vegetation cover for all seasons with *C*-value of 0.75 so the soil load at the outlet has a low value even though the area contributing to the silt load is high. The average slope of micro-watersheds varies from 4.5% to 8% and accordingly is a contributory factor for reduced silt load. Generally, there is an increase in soil load with increase in peak runoff except in the micro-watersheds where the cropping factor (*C*-value) is low. This could be due to prevention of sediment transport by the vegetation cover for different seasons. The continuous raster layers for the USLE parameters was integrated to get the silt load for each micro-watershed.

The run-off potential raster layer and soil erosion raster layer generated using the raster interpolation kriging method is given in Figure 5. Higher run-off potential (*Q*/*P*) is indicated by lighter tone in the run-off potential layer. The *Q*/*P* varies from 0 for most pervious surface to 1 for most impervious surface. The USLE soil erosion layer has also been generated using kriging interpolation. In case of USLE, darker tone of soil erosion layer indicates higher soil erosion area whereas lighter tone indicates lower soil erosion area. Both the raster layers have a resolution of 5 m.

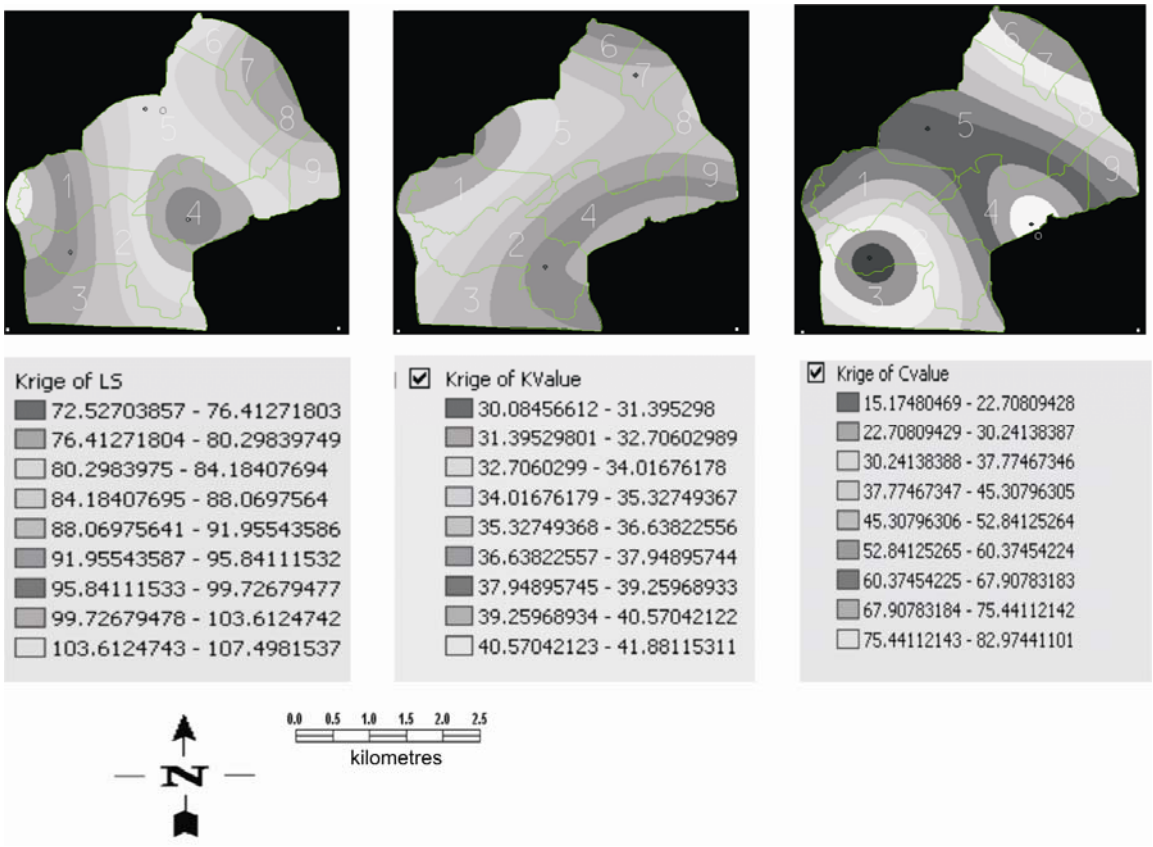

Figure 3. Raster interpolated layers for USLE parameters (variable search radius).

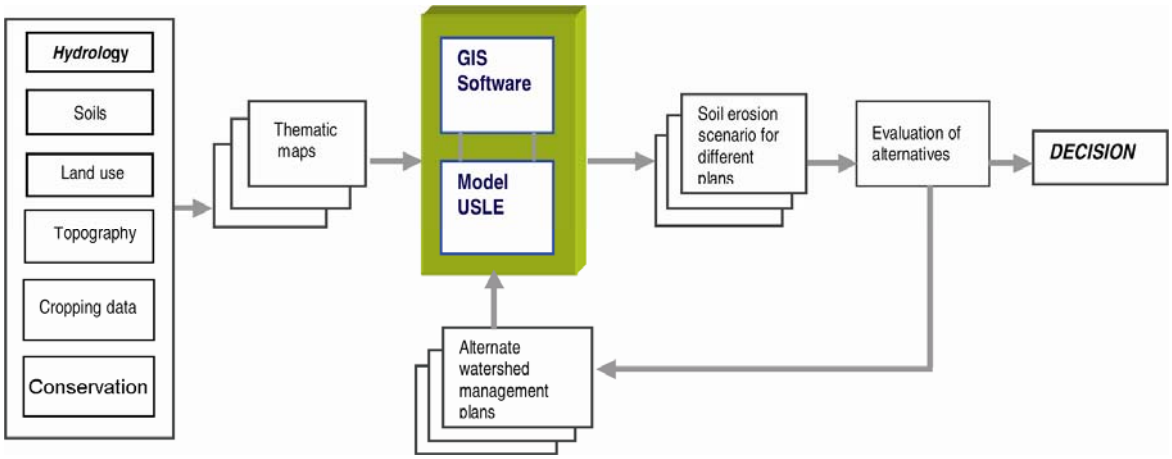

Figure 4. Concept diagram of the USLE for watershed management.

Validation of USLE silt load has been done by comparing it with the actual ground measurement of the total silt load in g per cubic cm and it is observed that the model estimates and measured values are in close agreement. Table 8 gives the details of the comparisons.

A general trend of positive correlation of annual silt load with peak runoff has been observed from the graph shown in Figure 6. The R^2 value is 0.0006, which is very less due to vegetation cover in the micro-watershed groups causing reduction of silt load. The plot on measured silt load and the model silt load shows positive correlation between them. The R^2 value is 0.0033. Low R^2 value could be attributed to nonconsideration of trap efficiency and delivery ratio at the site of actual measurement, accordingly the model estimates are higher than actual ground measurement near the outlets of the micro-

Table 5. *LS* factor for micro-watersheds

Micro-watershed no.	Total area	Contour length (m)	Average slope (*S*) %	Stream length (m)	Slope length (L)	$L * S$
1	3,163,265.30	12,735.8	8.05	3268.54	124.18	1.10
2	4,812,566.18	16,887	7.01	3250.71	142.49	0.98
3	4,469,674.83	14,643.4	6.55	2696.4	152.61	0.921
4	4,046,086.98	9,274.1	4.58	4000	218.13	0.70
5	7,601,434.56	21,339	5.61	3660.5	178.11	0.81
6	1,067,070.46	2,731.4	5.11	1307	195.33	0.76
7	1,109,329.55	3,853.3	6.94	1505	143.94	0.97
8	1,584,448.54	5,552.6	7.0	2535.9	142.67	0.98
9	1,476,105.52	4,465.3	6.05	1791	165.28	0.86

Table 6. Morphologic parameters and runoff for the micro-watersheds

Micro-watershed no.	*P* (m)	Area (sq. m)	Form factor	Drainage density	Ruggedness number	C_c	*Q*	Q_p
1	11,019.87	3,163,265.3	0.29	0.00406	2.66	0.32	119.72	6.3
2	14,405.96	4,812,566.2	0.45	0.00354	2.31	0.29	116.27	8.6
3	20,947.35	4,469,674.8	0.61	0.00327	2.16	0.12	118.55	9.0
4	12,921.68	4,046,087	0.25	0.00222	1.46	0.30	121.62	6.6
5	14,165.84	7,601,434.6	0.56	0.00283	1.82	0.47	119.45	13.0
6	4,648.723	1,067,070.5	0.62	0.00252	1.61	0.62	121.33	3.1
7	4,419.234	1,109,329.6	0.48	0.00344	2.04	0.71	119.33	3.1
8	6,886.857	1,584,448.5	0.24	0.00354	2.20	0.41	117.94	3.3
9	4,896.372	1,476,105.5	0.46	0.00305	1.90	0.77	118.35	3.5

C_c, Circulatory ratio; *Q*, SCS runoff (cm); Q_p, SCS peak runoff (cumec).

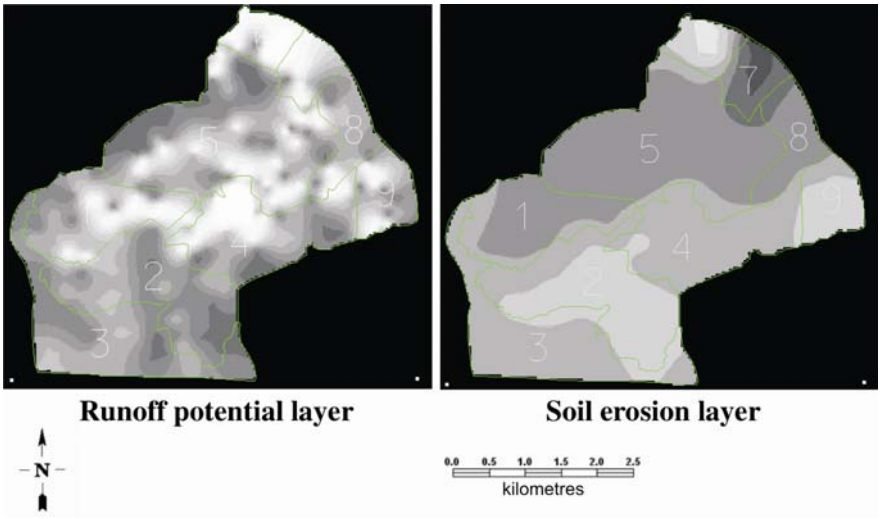

Figure 5. Run-off potential and soil erosion layer.

watershed groups. The GIS comparative assessment of micro-watersheds were supplemented with field visits to gather the following aspects in the study area.

- Hills and pediments with rocky outcrops with poor soil formation and can support only sparse vegetation.
- Steep slopes causing high erosion.
- Existing sparse vegetation of thorny scrubs provides very little protection against erosion.
- Rampant grazing has led to depletion of vegetative cover.
- Felling of trees to meet fuel wood demands.

The GIS spatial analysis carefully evaluated the different facets of terrain based upon their characteristics that were incorporated into the respective wastelands; the following measures can be suggested for improvement of the micro-watersheds.

Table 7. The USLE based annual silt load for the nine micro-watersheds

Micro-watershed no.	Total area	$L * S$	R-factor	K-factor	C-factor	P-factor	A (tonnes/hectare/year)	Priority
1	3,163,265.30	1.10	30.04	0.3	0.87	1	8.7	Moderate
2	4,812,566.18	0.98	30.04	0.33	0.75	1	7.3	Low
3	4,469,674.83	0.92	30.04	0.35	0.8	1	7.8	Moderate
4	4,046,086.98	0.70	30.04	0.39	0.92	1	7.6	Moderate
5	7,601,434.56	0.81	30.04	0.41	0.9	1	9.0	High
6	1,067,070.46	0.76	30.04	0.36	0.78	1	6.4	Low
7	1,109,329.55	0.97	30.04	0.42	0.87	1	10.7	High
8	1,584,448.54	0.98	30.04	0.39	0.8	1	9.1	High
9	1,476,105.52	0.86	30.04	0.34	0.82	1	7.3	Low

Table 8. Comparison of USLE based annual silt load for the nine micro-watersheds with ground measurements

Watershed no.	A (t/ha/year)	Measured silt load (g/cubic cm)	Model silt load (g/cubic cm)
1	8.70	0.04	0.07
2	7.29	0.02	0.06
3	7.79	0.05	0.06
4	7.62	0.04	0.06
5	9.07	0.05	0.07
6	6.44	0.02	0.05
7	10.68	0.02	0.08
8	9.19	0.02	0.07
9	7.26	0.02	0.06

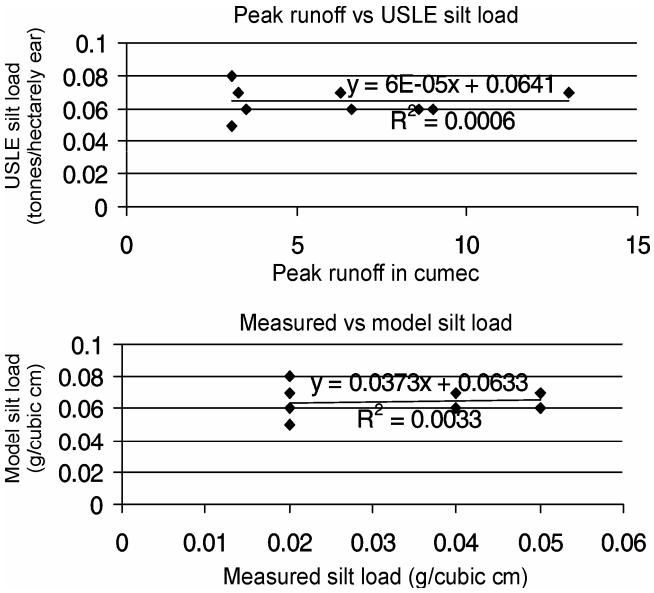

Figure 6. Plots on peak runoff versus USLE silt load and measured silt load versus model silt load.

- Introducing the management of natural resources – soil, water, vegetation through an integrated sustainable production system over the whole watershed.
- Land protection against wind and water erosion.
- Reclamation of wasteland through gully stopping.
- Improved vegetation cover and biodiversity.

Land degradation from water-induced soil erosion is a serious environmental problem affecting large areas of the agricultural landscape. Soil erosion is a complex phenomenon governed by a large number of factors, such as rainfall, topography, soil, land use and conservation measures. Scientific management of soil, water and vegetation resources on a watershed basis is essential to control soil erosion to tolerable levels and thus prevent land degradation and rapid silting of the water bodies. Watershed management involves decision making about use of available resources for various purposes. The watershed management programmes will be planned to ensure sustainability of the resources and to minimize the environmental issues. Decision-making process concludes with the selection of the optimal management plans required in effective and efficient means of decision support. GIS is emerging as a tool for managing natural resources like land and water. In watershed management, GIS is helpful in predicting the suitable management plans, prioritizing the watersheds for conservation and for presenting the results spatially for the decision-makers.

1. Rossiter, G. D., A theoretical framework for land evaluation. *Geoderma*, 1996, **72**, 165–190.
2. Sharma, R. and Rai, Y. K., *Integrated Watershed Management: Case Study in Sikkim Himalaya*, Gynodaya Prakashan, Nainital, India, 1992, pp. 4–11.
3. Band, L. E., Topographic partition of watershed with digital elevation models. *Water Resour. Res.*, 1996, **22**, 15–24.

4. Kumar, P., Kumar, S. and Manchanda, M. L., Satellite stereo data for DEM surfaces and derivatives. *J. Ind. Soc. Remote Sens*., 2004, **32**, 81–90.
5. Jenson, S. K. and Domingue, J. O., Extracting topographic structure from digital elevation data for geographic information system analysis. *Photogram. Eng. Remote Sensing*, 1988, **54**, 1593–1600.
6. Martz, L. W. and Garbrecht, J., Numerical definition of drainage network and the sub-catchment areas from digital elevation models. *Comp. Geosci.*, 1992, **18**, 747–761.
7. Vogt, J. V., Colombo, R. and Bertolo, F., Deriving drainage networks and catchment boundaries: a new methodology combining digital elevation data and environmental characteristics. *Geomorphology*, 2003, **53**, 281–298.
8. Saha, S. K., Prioritization of sub-watersheds based on erosion loss estimation – a case study of part of Song river watershed, Doon valley using satellite data. Proceedings of the National Symposium on Remote Sensing for Sustainable Development, 1992, pp. 181–186.
9. Rao, D. P., Gautam, N. C., Nagaraja, R. and Ram Mohan, P., IRS-1C application in land use mapping and planning. *Curr. Sci.*, 1996, **70**, 575–578.
10. Moore, I. D. and Wilson, J. P., Length-slope factors for the revised Universal soil loss equation simplified method of estimation. *J. Soil Water Conserv.*, 1992, **45**, 423–428.
11. Jasrotia, A. S., Rainfall–runoff and soil erosion modeling using remote sensing and GIS technique – a case study of tons watershed; paper in of photonirvachak. *J. Indian Soc. Remote Sensing*, 2002, **30**, 167–180.
12. Kothyari, U. C. and Jain, S. K., Sediment yield estimation using GIS. *Hydrol. Sci. J., Proc. IAHS*, 1997, **42**, 833–843.
13. Hydrology. In *SCS National Engineering Handbook*, USDA Soil Conservation Service, US Department of Agriculture, DC, 1972, section 4.
14. Singh, G., Venkataramanan, C., Sastry, G. and Joshi, B. P., *Textbook on Manual of Soil and Water Conservation Practices*, Oxford and IBH, New Delhi, 1990.

ACKNOWLEDGEMENTS. We thank the Dept of Environmental Science, Pune University for the technical and other support extended for the study; Prof. Ghole, Former Head of Environmental Science, University of Pune for giving his technical inputs and encouragement during the various phases of the work.

Received 6 January 2009; revised accepted 7 December 2009

ADP-glucose pyrophosphorylase activity in relation to starch accumulation and grain growth in wheat cultivars

Vaibhav D. Lohot, Poonam Sharma-Natu, Rakesh Pandey and M. C. Ghildiyal*

Division of Plant Physiology, Indian Agricultural Research Institute, New Delhi 110 012, India

ADP-glucose pyrophosphorylase (AGPase) activity in the developing grains of four wheat (*Triticum aestivum* L.) cultivars DL153-2, C306, HD2329 and WH542 grown under normal (27 November) and late (28 December) sown conditions was determined in relation to their grain growth and starch content. In order to analyse the temperature sensitivity of AGPase, excised developing grains (20 days after anthesis) of normal sowing were exposed for 1 h at 25°C, 35°C and 45°C and subsequently analysed for AGPase activity. AGPase activity in the developing grains was also determined in presence of PGA and Pi to evaluate the sensitivity of the enzyme to allosteric effectors. The study showed a highly significant correlation of AGPase activity with starch accumulation and grain growth in wheat under normal sowing but not so under late sowing. However, AGPase was not found to be that sensitive to moderate heat so as to be responsible for decreased starch accumulation and grain growth under late sowing. PGA helped in overcoming inhibition by Pi but did not activate the AGPase further. However, genotypic differences in the sensitivity of AGPase to allosteric effectors were observed. An efficient AGPase insensitive to regulation by PGA and Pi in wheat grain would lead to faster starch accumulation and early filling of grains and may thus avoid extreme terminal high temperature experienced during grain development.

Keywords: ADP-glucose pyrophosphorylase, grain growth, heat tolerance, starch, wheat.

STARCH constitutes around 70% of dry matter in wheat grain. Synthesis and deposition of starch may, therefore, be an important determinant of the size of the grain and thus directly have an impact on yield[1,2]. Starch in grains is deposited in amyloplasts involving ADP-glucose pyrophosphorylase (AGPase), starch synthases and branching enzymes[3,4]. A number of genetic and biochemical studies have established that AGPase is a rate limiting and regulatory enzyme in the pathway of starch synthesis[2,3,5]. AGPase is allosterically activated by 3-phosphoglycerate (3PGA) and inhibited by Pi. In fact, the ratio of 3PGA/Pi governs the catalytic activity of AGPase in leaves[2,6]. The extent to which this enzyme in non-photosynthetic tissues,

*For correspondence. (e-mail: mc_ghildiyal@rediffmail.com)